Geochemical and Petrogenesis of Granitoides rocks in South-East of Centeral Iranian Volcanic Belt, North-West of Share-Babak, Kerman Province, Iran

Gholamreza Ghadami[1]

1- Department of Geology, Faculty of science, University of Hormozgan, 3995 Bandar Abbass, Islamic Republic of Iran.

* Corresponding Author: ghadami@hormozgan.ac.ir

Received: 27 June 2016 / Accepted:24 December 2016 / Published online: 28 December 2016

Abstract

In the Centeral Iranian Volcanic Belt (CIVB), north-west of Shahre-Babak, in area of Javazm, Dehaj and khabr, about 20 plutonic porphyritic tonalitic to granodioritic masses (1-50 km2) are intruded into a varity of rock sequences from Eocene to Early Miocene in age. Tonalitic and granodioritic rocks are some part of Dehaj-Sardoieh belt and having early Miocene age. The CIVB contains intrusive and extrusive rockes of Cretaceous-Quaternary age. Geochemical studied indicate that the subalkalic tonalitic to granodioritic masses belong to I-type granitoides and have an adakitic composition tendency with Na_2O/K_2O (1.82-2.57), high Sr (584-1040 ppm), Mg#=(0.2-0.52) and low Y (7.3-10.7ppm), low Yb (0.7-1.18ppm), and low HREE. Fractionated REE patterns show that, $(Ce/Yb)_N$ = 10-22, absence of negative Eu anomaly, low content of Y, Nb, Ti, and high Sr/Y (74-134) and $(Ce/Yb)_N$ ratios. Based on geochemical data the source of tonalitic and granodioritic magma was probably garnet-amphibolite or amphibole-eclogite, possibly generated during subduction of the Neo-Tethyan oceanic slab beneath the Central Iran microplate. The adakitic plutonism was followed by adakitic volcanism in Mio-Peliocene and eruption of alkaline magmatism in this area. The thermal needs for slab melting results the shear stress of oblique convergent. The tectonic setting of tonalitic and granodioritic masses are an active continental margin and belong to volcanic arc granitoides.

Keywords: Adakite; Tonalite; Granodiorite; Neo-Tethys; Iran.

1- Introduction

The Tethyan orogenic collage formed from collision of dispersed fragments of Gondwana with Eurasia (Ghasemi and Talbot, 2006). Within this context, three major tectonic elements with NW-SE trends are recognized in Iran due to collision of Afro-Arabian continent and Iranian microcontinent (Mohajjel *et al*., 2003). They include the Central Iranian Volcanic Belt (CIVB), Sanandaj-Sirjan metamorphic zone and Zagros-folded-thrust belt (Fig.1) (Mohajjel *et al*., 2003; Shahabpour, 2007). The CIVB are contains intrusive and extrusive rocks of Cretaceous -Quternary age that forms a belt with 50 Km wide and 4 Km thick (Berberian and Berberian, 1981) that extends from NW to SE in Iran. However, peak of magmatic activity is thought to be Eocene age (Alavi, 2004). Geochemical studies indicate that the CIVB is generally composed of alkaline and calc-alkaline rocks. For examples alkaline rocks also are reported locally by Amidi *et al*., (1984) and Moradian, (1997). Amidi *et al*., (1984) proposed a rift model to interpret the genesis of Eocene magmatic rocks in the CIVB. Berberian and King (1981) argued that the onset of alkaline volcanism, which followed the calc-alkaline volcanism (6-5 Ma) in CIVB was due to sinking of the final broken pieces of oceanic slab to a depth where alkaline melts were generated (Jahangiri, 2007). The post-suturing magmatic activity along the Sanandaj-Sirjan zone and NW Iran can be attributed to slab break-off (Jahangiri, 2007).

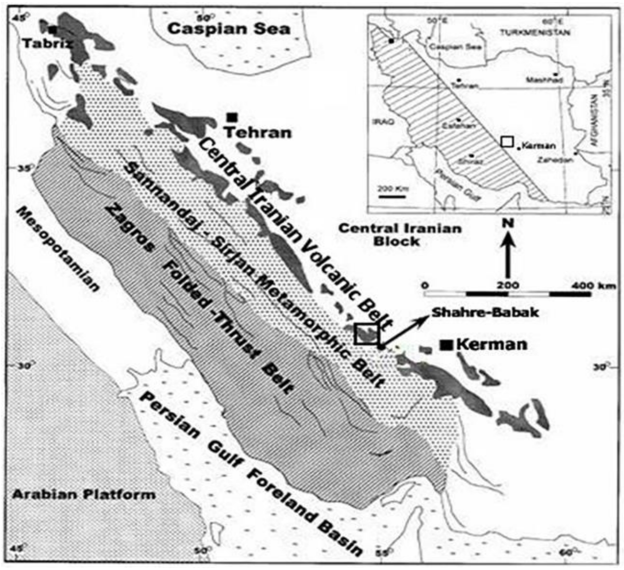

Figure 1) Three main tectonic units of the Zagros orogenic belt (Mohajjel et al., 2003). Studied area is marked by square.

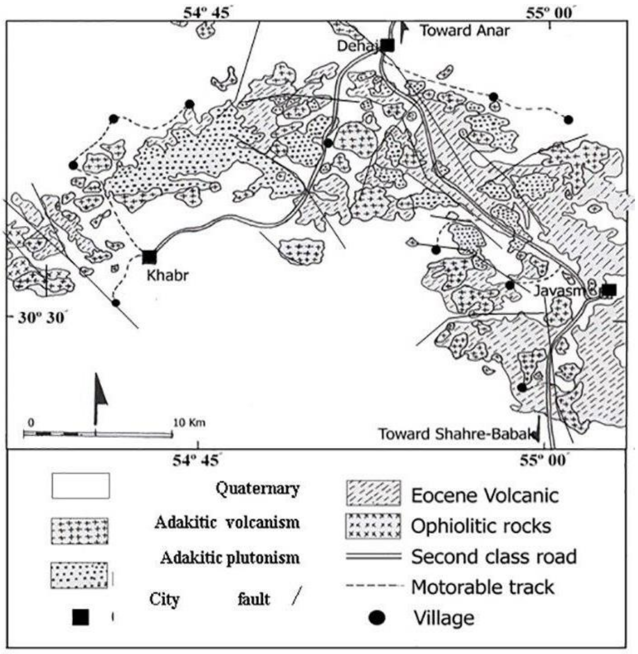

Figure 2) Geological map of area (Simplified from the geological map of 1: 250000 Anar), (Dimitrijevic et al., 1971).

In CIVB, north-west of Shahre-Babak, area of Javazm, Dehaj and Khabr a geologic complexity and magmatic activity from calc-alkaline to alkaline presented (Ghasemi and Talbot, 2006). The diversity of magmatic types from calk-alkaline to alkaline indicate region of Javazm, Dehaj and Khabr to reperesent classical areas of young volcanism. The most intense eruptions were during the post collisional stage, which led to the formation of great volcanoes like Masahim (Mozahem), Madvar, Aj Bala, Aj Pain and other volcanoes in this region (Hassanzadeh, 1993).

The great diversity of Neogene to Quaternary magmatic rocks, from granitoides andesitic, dacitic to rhyodacitic subvolcanic domes (Ghadami *et al*., 2008; Ghadami, 2009) and extending for more than 150 km, are of interested due to their specific conditions of formation and spatial and temporal relation with other magmatic rocks. The tonalite-granodiorite plutonism of Miocene in this area is followed by adakitic volcanism in Mio-Peliocene (Ghadami *et al*., 2008; Ghadami, 2009) and alkaline volcanism in Plio-Quaternary (Amidi *et al*., 1984). A conspicuous characteristic of this phase is the contemporaneous eruptions of mafic alkaline melts including melafoidites and alkali basalts (Berberian, and King, 1981).The temporal and spatial relationship of calc-alkaline (adakitic) magmatism with alkaline volcanism is also reported from different areas of Gondwana fragments and Eurasia plate collision zone (Chung, *et al*., 2005; Sajona, *et al*., 2000).

The aims of this paper are (1) to present chemical characteristics of the tonalite-granodiorite plutonism in Central Volcanic Belt of Iran, (2) to suggest the conditions of their genesis, and (3) to discuss geodynamic environment in which they could have formed.

2- Material and methods

2.1- Regional Setting

The investigated area is situated at the Central Iranian Volcanic Belt (CIVB), north-west of Shahre-Babak City (Fig. 1-2), betwen Rafsanjan fault and Nain-Baft fault (Shahre-Babak fault). In this area, numerous (n≈20) tonalite-granodiorite masses are intruded in to the volcanic Eocene, Oligocene and volcanosedimentary rocks of Central Iranian Volcanic Belt (Dimitrijevic *et al*., 1971, Fig. 2).

In the studied area the Eocene volcanic and volcanoclastic rocks consist of basalt, andesitic-basalt, brecciated volcanoclastic rocks and green tuffs (Fig. 2). The age of emplacement of tonalitic and granodioritic rocks are Miocene (Dimitrijevic *et al*., 1971).

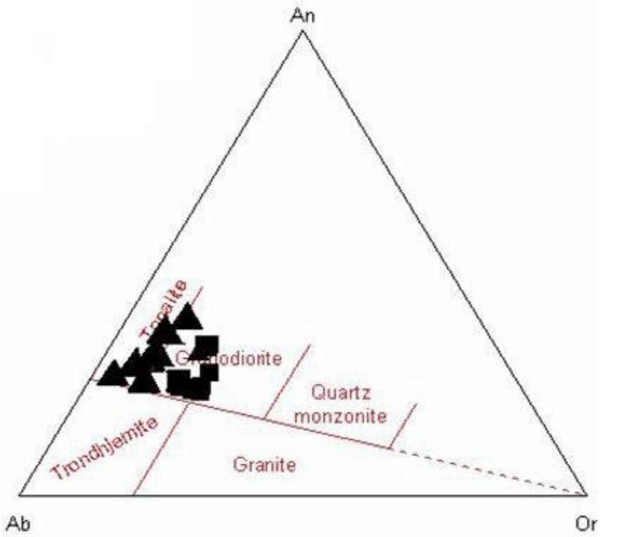

Figure 3) Classification of granitoides rocks. The studied samples compositions range from Tonalites ▲ to Granodiorites ■ (Cox et al., 1979).

2.2- Petrographic features

The porphyritic plutonic masses consist of intermediate to felsic suites whose composition varies from tonalite to granodiorite (Fig. 3). Tonalite and granodiorite rocks show porphyritic texture with phenocrysts of plagioclase, hornblende and biotite. Plagioclase is ubiquitous phenocrysts (25-50 vol %) and contains inclusions of magnetite, amphibole and opaque. These rocks contain large plagioclase crystals (3-5mm) that usually exhibit sieve textures and well defined zoning marked by concentric zones rich in/or devoid of opaque inclusion. In some samples, plagioclase phenocrysts are mantled by a clouded or solved rim. These features show that the magma mixing or effective of volatiles pressure (H_2O) in orogenic magmatic belts (Gill, 1981).

Hornblende occurs as the main ferromagnesian phenocrysts (up to 2 mm) in tonalite and granodiorite and varies from green to brown in color. In some samples, accumulation of hornblende led to formation of glomeroporphyric texture. The groundmass is composed of plagioclase and hornblende as the main minerals, with apatite, biotite, quartz and iron oxides as accessory minerals.

2.3- Geochemical characteristics

2.3.1- Analytical methods

Based on petrographic studies, 12 samples of tonalite and granodiorite rocks were chosen for major, trace and rare-earth elements (REE) analysis. Samples for whole rock analysis were crushed and powdered in agate ball-mills. Major elements were determined by ME-ICP method. Inductively Coupled Plasma-Mass Spectorometry (ICP-MS) was employed for REE and trace element analysis for all of the samples. All of the analysis work was determined at ActLabs laboratories (Canada). Representative chemical analysis for major, trace and rare earth elements are presented in Table 1.

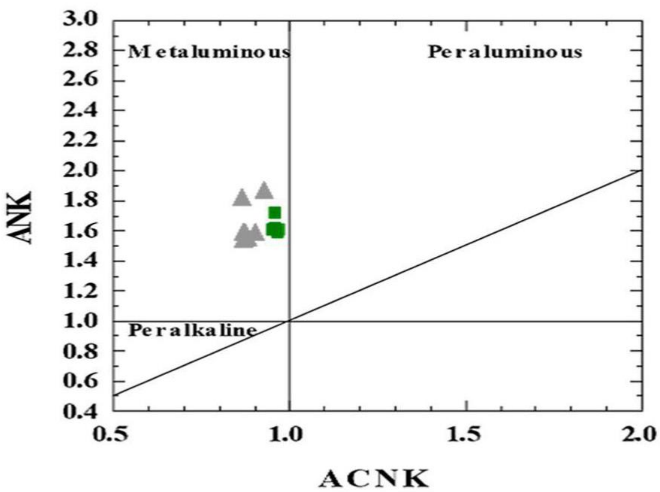

Figure 4) A/CNK vs. A/NK diagram, all of the samples of granitoides plot in metaluminous filed, A/CNK=[Al_2O_3]/[$CaO+Na_2O+K_2O$], A/NK= [Al_2O_3]/[Na_2O+K_2O] (Maniar and Piccoli, 1989; Symbols is same as Fig. 3).

2.3.2- Analytical results

The SiO_2 of samples vary from 58.8 to 65.5 wt %. Using ternary diagram of Ab-An-Or (Cox *et al.*, 1979), for classification of plutonic rocks, the studied samples plot in the fields of granodiorite and tonalite (Fig. 3). Also these rocks are metaluminous with Al_2O_3/ (CaO+Na_2O+K_2O) ratios of 1.5-2.0 (Fig. 4). Using SiO_2 as a fractionation index, the samples display chemical variation and clear trends on Harker diagrams (Figs. 5-7). On variation diagram, MgO, CaO, FeO_t, TiO_2, MnO and P_2O_5 display negative correlations. Also compatible rare elements of V, Co, Cr and Ni display negative correlations (Fig. 6).

Incompatible elements of Zr, Hf, Cs and Pb display positive correlation. These feathers which suggesting that the granodiorite and tonalite rocks experienced fractionation of hornblende, plagioclase and apatite (Fig. 7). The other oxides and elements (e.g. K_2O, Na_2O, Rb, Ba, Sr and etc.) were displayed scatter trends. The scattered of the samples belong to present of phenocrysts (fractional crystallization) or assimilation of continental crust. In diagram of Na_2O+K_2O vs. SiO_2 (Irvine and Baragar, 1971) all samples were located in the subalkaline field (Fig. 8). In SiO_2 vs. K_2O diagram (Pearce, 1982), all of the samples plot in calc-alcaline magmatic series (Fig. 9). In the AFM diagram of (Irvine and Baragar, 1971) all of the samples show a calc-alcaline trend (Fig. 10). In K_2O vs Na_2O diagram (White and Chappel, 1983) all of the samples plot in I-type field (Fig. 11).

***Table 1**) Representative chemical analysis for major oxides, trace and rare earth elements*

Sample	14-1	14-6	23-1	26-6	29-4	37-2	39-2	41-2	43-2	44-3	45-2	70-3
Rock type	TO	TO	TO	TO	TO	GD	GD	GD	TO	GD	TO	GD
SiO_2	64.5	63.6	63	62.7	64	68.3	65.8	67.5	59.5	65.1	58.8	64.5
Al_2O_3	16.45	16.45	16	16.55	16.55	16.25	15.85	16.35	17.6	16.35	17.2	16
Fe_2O_3*	3.51	3.62	3.49	4.1	3.93	2.22	3.16	3.02	5.33	3.61	5.41	3.54
CaO	4.35	4.69	4.37	4.59	4.77	3.32	3.76	3.39	5.26	3.56	5.8	3.47
MgO	1.29	1.32	1.74	1.81	2.14	0.28	1.17	0.62	2.22	1.34	2.98	1.27
Na_2O	5.01	5	4.91	4.93	5.07	4.72	4.21	4.76	4.34	4.75	4.43	4.57
K_2O	1.95	2.01	2.04	2.41	1.91	2.46	2.31	2.38	2.09	2.4	1.98	2.38
Cr_2O_3	0.03	0.02	0.02	0.03	0.02	0.03	0.02	0.02	0.02	0.02	0.03	0.01
TiO_2	0.42	0.44	0.44	0.52	0.48	0.42	0.41	0.4	0.56	0.4	0.53	0.37
MnO	0.05	0.07	0.06	0.07	0.06	0.01	0.05	0.03	0.08	0.06	0.08	0.05
P_2O_5	0.2	0.21	0.2	0.24	0.19	0.17	0.18	0.17	0.22	0.17	0.21	0.16
LoI	1.94	2.28	1.65	1.34	0.81	1.44	3.02	1.2	2.34	2.07	2.3	2.04
Total	99.9	99.9	98.1	99.5	100	99.8	100	100	99.8	100	99.9	98.6
Na_2O/K_2O	2.57	2.49	2.41	2.05	2.65	1.92	1.82	2	2.08	1.98	2.24	1.92
K_2O/Na_2O	0.39	0.4	0.42	0.49	0.38	0.52	0.55	0.5	0.48	0.5	0.45	0.52
Na_2O+K_2O	7.09	7.16	7.19	7.44	7.03	7.28	6.72	7.21	6.59	7.28	6.57	7.19
FeO	1.18	1.8	1.8	2.08	1.98	1.12	1.62	1.52	2.72	1.83	2.76	1.86
Fe_2O_3	1.18	1.8	1.8	2.08	1.98	1.12	1.62	1.52	2.72	1.83	2.76	1.86
Mg#	0.43	0.43	0.48	0.48	0.53	0.2	0.43	0.30	0.46	0.42	0.52	0.41
S.I.	10.9	11	14.3	13.7	16.4	2.9	10.7	5.8	15.9	11	20.1	10.7
R.	61.5	59.9	61.5	61.5	59.4	68.4	63.5	67.8	55	66	52.5	66.7
	ppm	ppm	ppm	ppm	ppm	ppm	ppm	ppm	ppm	ppm	ppm	ppm
Ba	680	730	678	701	650	845	632	620	955	798	741	739
Cr	230	170	150	190	130	200	100	140	140	110	220	110
Cs	0.87	0.62	1	1.04	0.56	3.08	2.52	1.65	1.11	2.42	1.54	2.29
Cu	40	38	42	49	35	17	38	42	23	16	58	14
Ga	20.4	21	20.7	21.5	20.3	20.2	20	21	21	18.9	19.9	18
Hf	3.1	3.2	3.2	3.5	3.3	4.2	3.8	3.8	3.3	3.6	3.4	3.4
Mo	7	5	2	3	4	7	4	3	5	3	5	3
Nb	5.5	6.9	7.5	7.1	4.9	6.4	5.3	5.4	4.9	4.7	4.5	4.3
Ni	21	19	24	27	32	12	14	16	20	13	42	10
Pb	12	10	13	14	12	47	15	16	16	16	27	15
Rb	38	37.8	39.5	50.6	38.7	63.5	59.9	59.9	52.2	63	49.4	58.9
Sr	1010	1040	1005	1000	967	584	645	624	947	1020	891	970
Ta	0.5	0.6	0.6	0.6	0.5	0.7	0.6	0.6	0.6	0.5	0.5	0.4
Th	4.97	6.84	8.73	6.62	3.94	7.7	6.94	6.43	9.11	7.32	8.98	7.01
U	1.64	2.08	2.36	1.87	1.39	2.42	2.34	2.4	2.88	2.22	2.9	2.07

Table 1) Continued.

Sample	14-1	14-6	23-1	26-6	29-4	37-2	39-2	41-2	43-2	44-3	45-2	70-3
Rock type	TO	TO	TO	TO	TO	GD	GD	GD	TO	GD	TO	GD
V	76	80	78	94	88	61	64	62	130	74	126	68
W	7	5	8	10	5	7	3	9	7	3	6	3
Y	7.5	9.1	8.6	10	9.3	7.8	8.5	7.7	9.8	8.5	10.7	8.2
Zr	110	116	126	132	108	147	133	136	109	126	113	120
Ti	2520	2640	2640	3120	2880	2520	2460	2400	3360	2400	3180	2220
P	873	916	873	1047	829	742	785	742	960	742	916	698
Rb/Sr	0.04	0.04	0.04	0.1	0.04	0.11	0.09	0.1	0.06	0.06	0.06	0.06
Sr/Y	134.7	114.3	116.9	66.2	104	74.9	75.9	81.81	96.9	120	83.3	118.3
Sr/Ba	1.49	1.42	1.48	0.94	1.49	0.69	1.02	1.01	0.99	1.28	1.20	1.31
Rb/Ba	0.06	0.05	0.06	0.09	0.06	0.08	0.09	0.1	0.05	0.08	0.07	0.08
La	23.07	33	33.4	29.2	20.6	25.7	25.6	23.5	24.9	21.3	24.8	21
Ce	45.1	60.2	61.5	54.9	40.3	47.9	46.8	44.7	43.1	39.6	44.3	38.7
Pr	4.8	6.17	6.11	5.86	4.46	4.91	4.95	4.69	4.55	4.16	4.62	4.38
Nd	17.6	21.9	21.6	21.6	17.4	17.8	17.8	17.2	16.9	15.5	17.5	16.8
Sm	3.15	3.69	3.65	3.74	3.27	3.42	3.36	3.23	3.2	3.02	3.52	2.75
Eu	0.95	1.08	1.06	1.07	0.99	0.99	1.1	0.98	1.01	0.93	1.16	0.82
Gd	2.71	3.1	3.1	3.24	3.04	3.15	3.11	3.18	2.89	2.77	3.29	2.52
Tb	0.31	0.4	0.34	0.43	0.37	0.38	0.44	0.41	0.39	0.39	0.46	0.32
Dy	1.57	1.92	1.78	2.06	1.94	1.61	2.02	2.03	2.17	1.87	2.24	1.58
Ho	0.28	0.34	0.3	0.33	0.36	0.3	0.35	0.33	0.39	0.34	0.45	0.28
Er	0.81	0.92	0.91	1.07	1.02	0.83	1.07	0.97	1.2	1.05	1.3	0.83
Tm	0.09	0.11	0.1	0.14	0.14	0.11	0.14	0.15	0.15	0.15	0.2	0.1
Yb	0.7	0.77	0.82	0.96	0.95	0.75	1.03	0.9	1.08	0.9	1.18	0.71
Lu	0.1	0.11	0.12	0.13	0.12	0.11	0.14	0.15	0.15	0.14	0.17	0.1
Zr/Nb	20	16.8	16.8	20.9	22	22.9	25	25.1	22.2	26.8	25.1	27.9
La/Sm	7.5	8.9	9.1	8.6	6.3	7.5	7.7	7.3	7.8	7	7	7.6
Sm/Yb	4.5	4.8	4.4	3.5	3.4	4.6	3.3	3.6	2.9	3.4	2.9	3.9
La/Yb	33.9	42.9	40.7	30.4	21.6	34.3	24.9	26.1	23	23.7	21	29.6
Ba/La	28.7	22.1	20.3	24	31.5	32.9	24.7	26.4	38.4	37.4	29.9	35.1
La/Nb	4.3	4.8	4.4	4.6	4.2	4	4.8	4.3	5	4.5	5.5	4.9
La/Th	4.8	4.8	3.8	4.2	5.2	3.3	3.7	3.6	2.7	2.9	2.8	3
Th/Yb	7.1	8.9	10.6	7.2	4.1	10.2	6.8	7.1	8.4	8.1	7.6	9.9
(La/Yb)N	24.39	31	29.25	21.84	15.54	24.64	18	18.72	16.54	16.98	15	21.1
(Ce/Yb)N	18	21.9	20.85	15.9	11.8	17.8	12.75	13.8	11.09	12.21	10.34	15.5
∑REE	101	133.7	134.8	121	94.96	108	108	102.5	102	92.12	105.2	90.86

Figure 12 show spider diagrams plot for representative samples from different plutonic masses normalized to Conderite and N-MORB composition (Sun, and McDonough, 1989). The tonalite and Granodiorite rocks are enriched in large ion lithophile elements (LILE) such as K, Rb and Ba and Sr relative to HFSE, and negative Ti, Zr, Y and Nb anomalies. They show significant positive anomalies for Sr, indicative of either the absence of plagioclase fractionation or retention of plagioclase in the residue (Green *et al.*, 1989; Pearce and Parkinson, 1993; Rapp, *et al.*, 1999). LILE and LREE enrichment can result from low degree partial melting of the MORB source. Decoupling of Zr and Ti with similar bulk Kd's and greater depletion of Ti has been interpreted to reflect a residual phase in the source that fractionated Ti (Pearce and Parkinson, 1993), or Ti-bearing phases (Reagan, and Gill, 1989). The strong depletion of Y and Yb corresponds to presence of amphibole or restite garnet in the source melting (Pearce and Parkinson, 1993). These geochemical features show that all of the granodiorite and tonalite rocks exhibit typical subduction-related signatures.

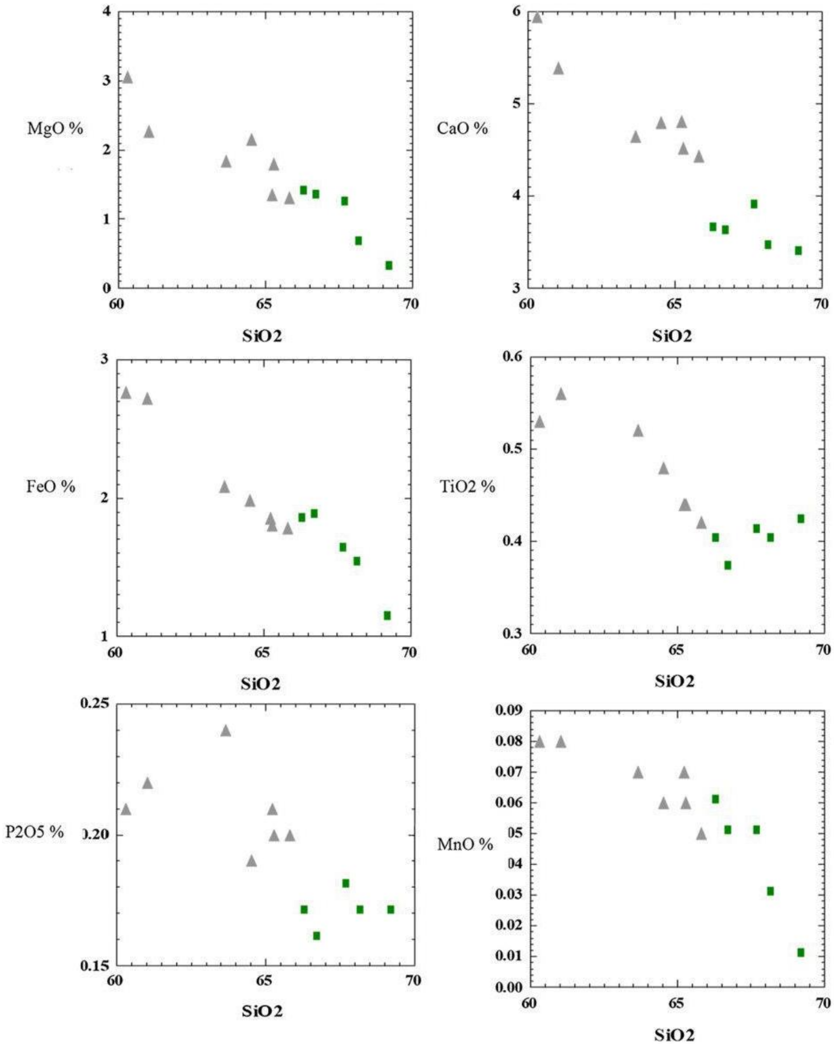

Figure 5) Variation diagrams for major and trace elements of samples (Symbols is same as Fig. 3).

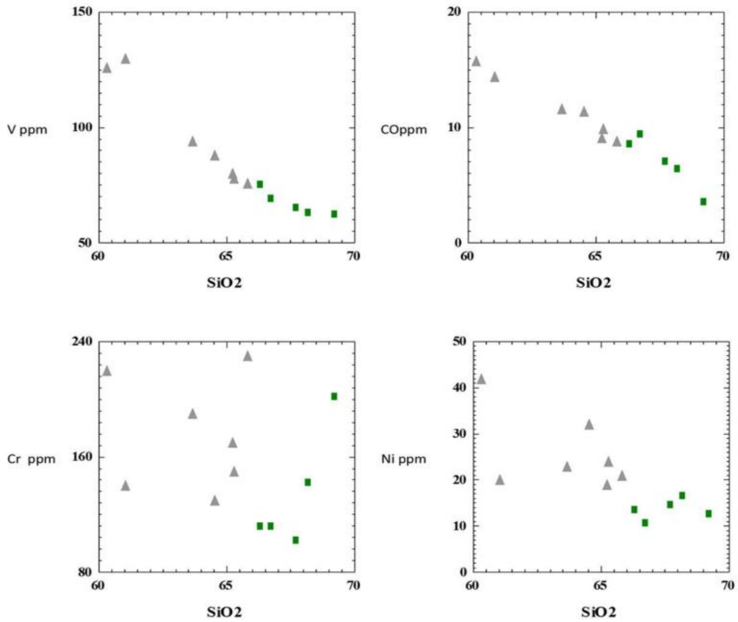

Figure 6) Continue of variation diagram (Symbols is same as Fig. 3).

The REE concentrations samples of granodiorite and tonalite rocks from studied area are plotted relative to Chondrite and N-MORB in figure 13. The ∑REE ranges from 92.1 to 134.8 ppm. The REE patterns for adakitic rocks from the study area are similar, although the abundances are variable. All the samples are enriched in LREE and strongly fractionated in LREE and have a flat MREE to HREE pattern (La_N/Yb_N values of 15.5 to 29.2). The REE patterns are linear with a small positive Eu anomaly, implying their cogenetic nature and derived from source regions that had similar relative concentrations of REE and similar mineralogy. Low abundances of HREE in granodiorites and tonalities rocks reflect retention of these elements in residual garnet in the partially melted subducted slab of amphibole-eclogite (Green *et al.*, 1989). There are no cross-cutting REE pattems, suggesting that the studied magmatic suites are possibly related to and most likely derived from the same initial melt.

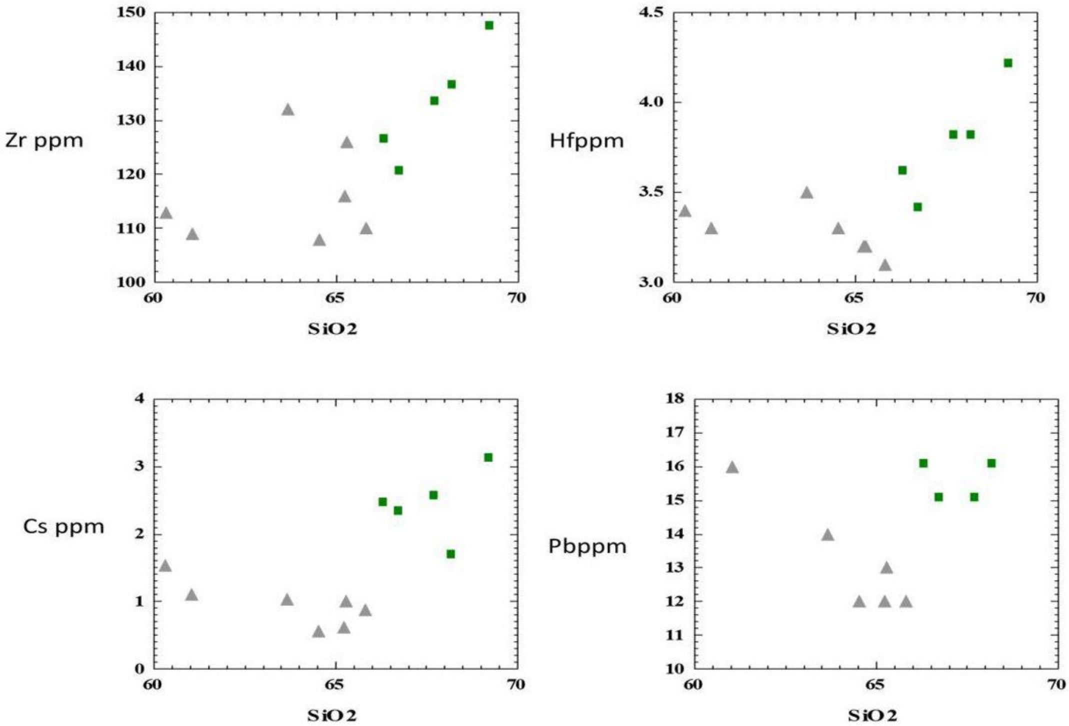

Figure 7) Continue of variation diagram (Symbols is same as Fig. 3).

In the Y vs. Sr/Y diagram, (Fig. 14A) all of the granodiorites and tonalites samples plot in the field of adakite relative to typical arc-related calc-alkaline rocks defined by (Defant and Drummond, 1990; Defant and Kepezhinskas, 2001; Martin *et al.*, 2004; Martin, and Hugh Rollinson, 2005; Oyarzun *et al.*, 2002). In the $(La/Yb)_N$ vs. Yb_N diagram, (Fig. 14B) all of the studied samples plot in the field of adakite relative to classical island arc rocks defined by (Defant and Drummond, 1990; Defant and Kepezhinskas, 2001; Martin *et al.*, 2004; Martin, and Hugh Rollinson, 2005; Oyarzun *et al.*, 2002). The Mg#[MgO/(MgO+FeO)] of the granodiorites and tonalites samples ranges from 0.2 to 0.52 and contains high concenteration of Sr (584 to 1040 ppm) and low contents of Y and Yb.

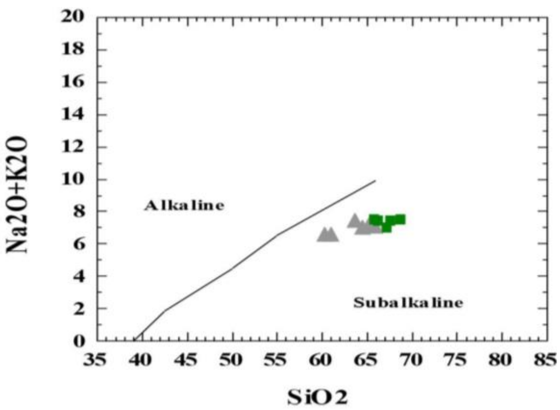

Figure 8) Diagram of SiO_2 vs. Na_2O +K_2O, all of the samples plot in subalkaline field, (Irvine and Baragar, 1971; Symbols is same as Fig. 3).

The high contents of Sr, high ratios of K_2O/Na_2O (0.39 to 0.55), Mg#(mean 0.42) and concentrations of Yb and Y indicate geochemical characteristics different from typical volcanic rocks and similar to adakitic rocks (Defant and Drummond, 1990; Defant and Kepezhinskas, 2001; Martin *et al.*, 2004; Martin, and Hugh Rollinson, 2005). The adakites exhibit Sr enrichment, in contrast to non-adakitic tonalite and granodiorite which show positive anomalies in spider diagrams.

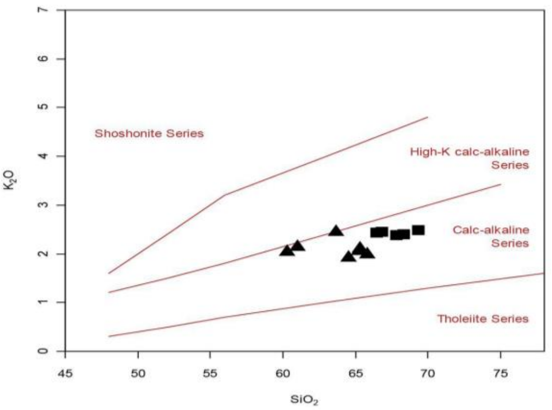

Figure 9) Diagram of SiO_2 vs. K_2O (Pearce, 1982), all of the samples plot in Calc-alkaline Series; Peccerillo and Taylor, 1976; Symbols is same as Fig. 3).

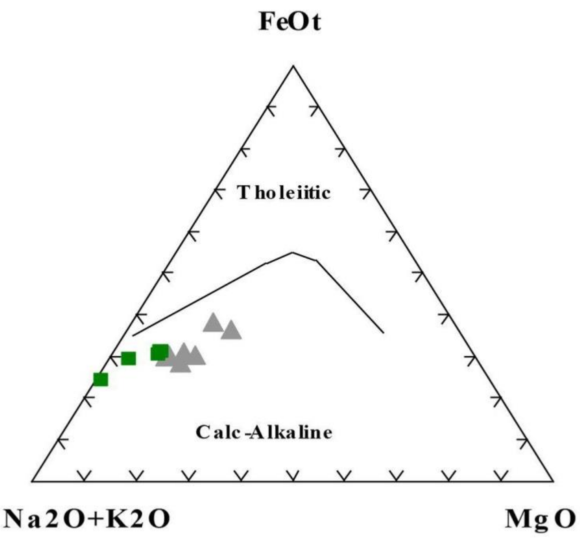

Figure 10) AFM diagram, all of the samples plot in Calc-alkaline Series field, (Irvine and Baragar, 1971; Symbols is same as Fig. 3).

In Shandl and Gorton diagrams (Haschke and Guenther, 2003; Oyarzun *et al.*, 2002), all of the granodiorites and tonalites samples plote in Active Continental Margins (Fig. 15). In Pearce *et al.* (1989) diagrams, all of the studied samples plotted in Volcanic Arc Granites (Fig. 16).

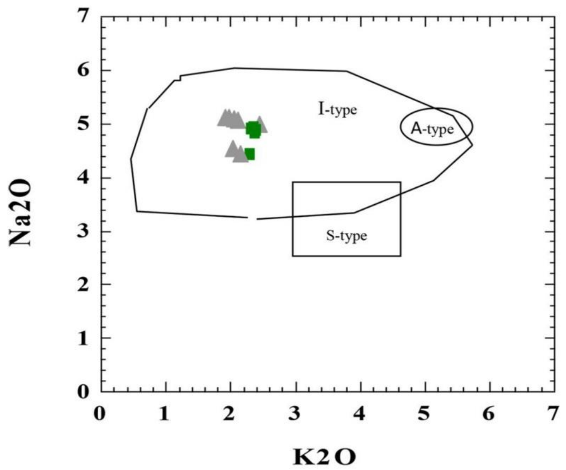

Figure 11) K_2O vs. Na_2O diagram (White and Chappel, 1983), all of the samples plot in I-type field Symbols is same as Fig. 3).

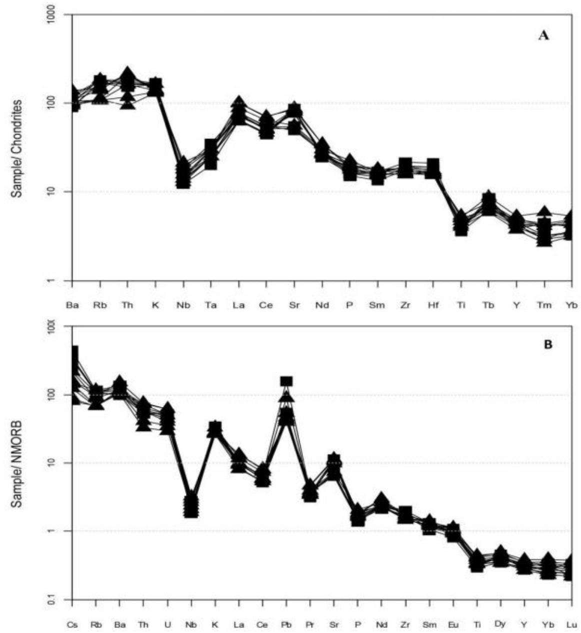

Figure 12) Chondrite-normalized REE patterns and N-MORB-normalized spidergrams for incompatible and trace elements (Sun and McDonough, 1989; Symbols is same as Fig. 3).

In diagram of Nb vs. Rb/Zr (Brown *et al.*, 1984) the studied samples plot in Continental Arc field (Fig. 17). In Batchelor and Bowden diagrams (1985), the studied granitoides of studied area plot in field of Pre-Plate Collision and Calc-alkaline series (Fig. 18). Diagram of Sm/Yb vs. La/Sm (Haschke, and Guenther, 2003; Kay and Mpodozis, 2002) shows mineralogy of source melting, the samples of studied area that show amphibole and garnet present in the source melting of this rocks (Fig. 19).

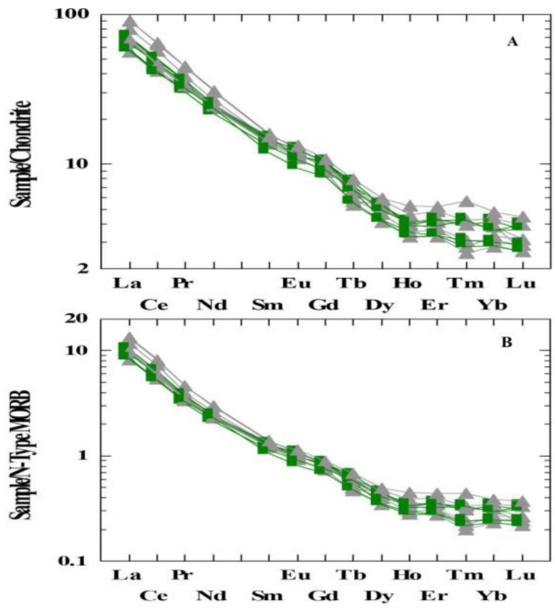

Figure 13) Chondrite-normalized REE patterns and N-MORB-normalized spidergrams for REEs (Sun and McDonough, 1989; Symbols is same as Fig. 3).

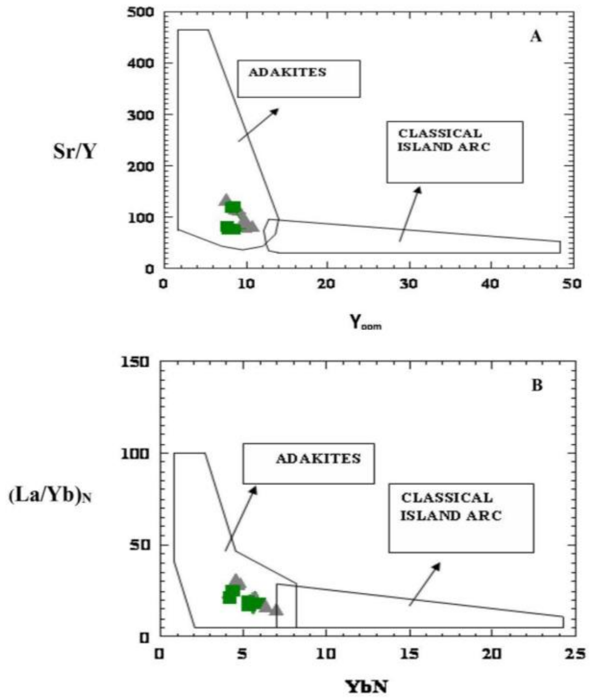

Figure 14) Y vs. Sr/Y (Defant and Drummond, 1990) and B) (La/Yb)N vs. YbN diagrams, discriminating between adakitic and classical arc calc- alkaline compositions, (Martin et al., 2004; Oyarzun et al., 2002; Reagan, and Gill, 1989; Symbols is same as Fig. 3).

In diagram of the Th vs. Th/Ce (Condie, 1989), all of the studied samples of granitoides plot in slab-drived adakites field (Fig. 20).

Therefore analytical results show granitoides rocks of studied area that formed in a volcanic arc or active continental margin related to subduction zone, and have adakitic affinity in compositions. Furthermore, amphibole and garnet were persent in the source of this rocks and plagioclase absent.

The Sr^{87}/Sr^{86} granitoidoides rocks of studied area are 0.704260 to 0.704443 (Ghadami, 2009), that show this adakitic rocks relative to slab-drived or MORB source (Martin *et al.*, 2004).

3- Discussion and conclusions

3.1- Discussion

The degree to which anatexis of subducted oceanic crust has contributed to magmatism in convergent plate margins has been a point of controversy for decades (Derek *et al.*, 2004; Gill, 1981). As discussed by Gill (1981), arc magmas of basaltic composition are regarded as products of mantle, not slab anatexis, although some later workers continued to press for slab anatexis in the production of arc basalts, particular those with high Al-contents (Martin, and Hugh Rollinson, 2005). Hydrated mantle peridotite as the principal source for arc basalts is now firmly established (Tatsumi and Koyaguchi, 1989), but genesis of intermediate and felsic are magmas remains controversial.

The issue of slab anatexis as a globally important process was emphasized by Defant and Drummond (1990) and Martin *et al.* (2004) who demonstrated a connection between subduction of young oceanic crust and production of intermediate to felsic igneous rocks which bear the signature of a garnetiferous residuum. Such magmatic rocks are compositionally similar to Tertiary lavas on Adak Island in the Aleutian arc which was identified as products of slab melting by Le Maitre *et al.*, (1989).

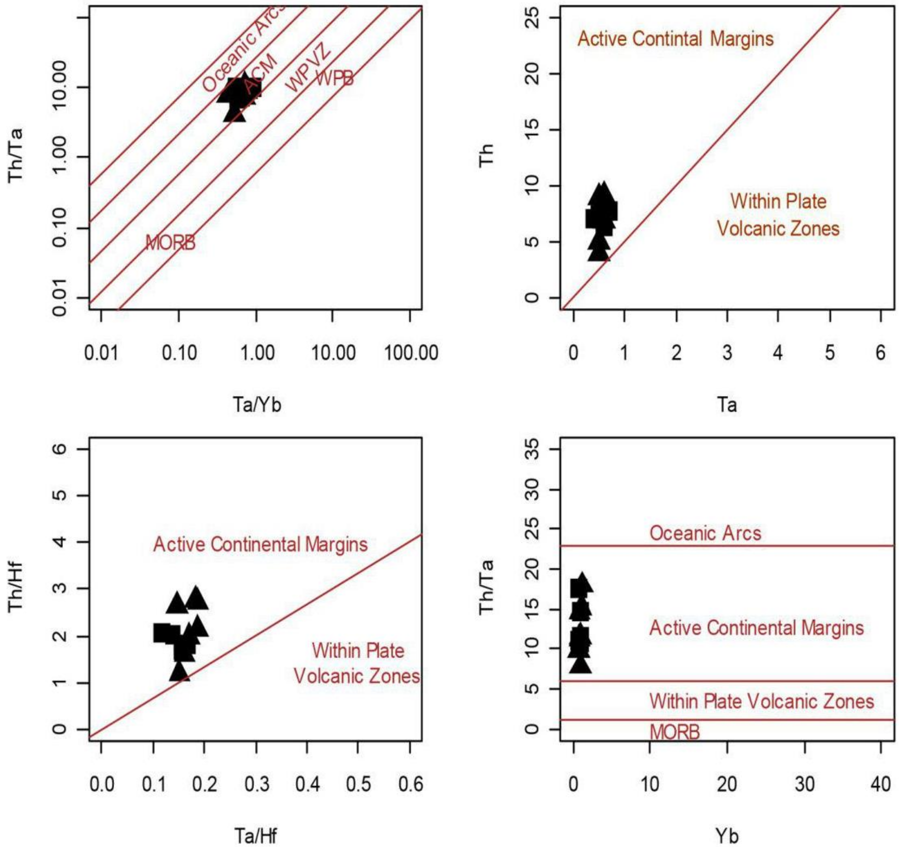

Figure 15) Schandl and Gorton (2002) diagrams, all of the samples plot in Active Contintal Margins; Symbols is same as Fig. 3).

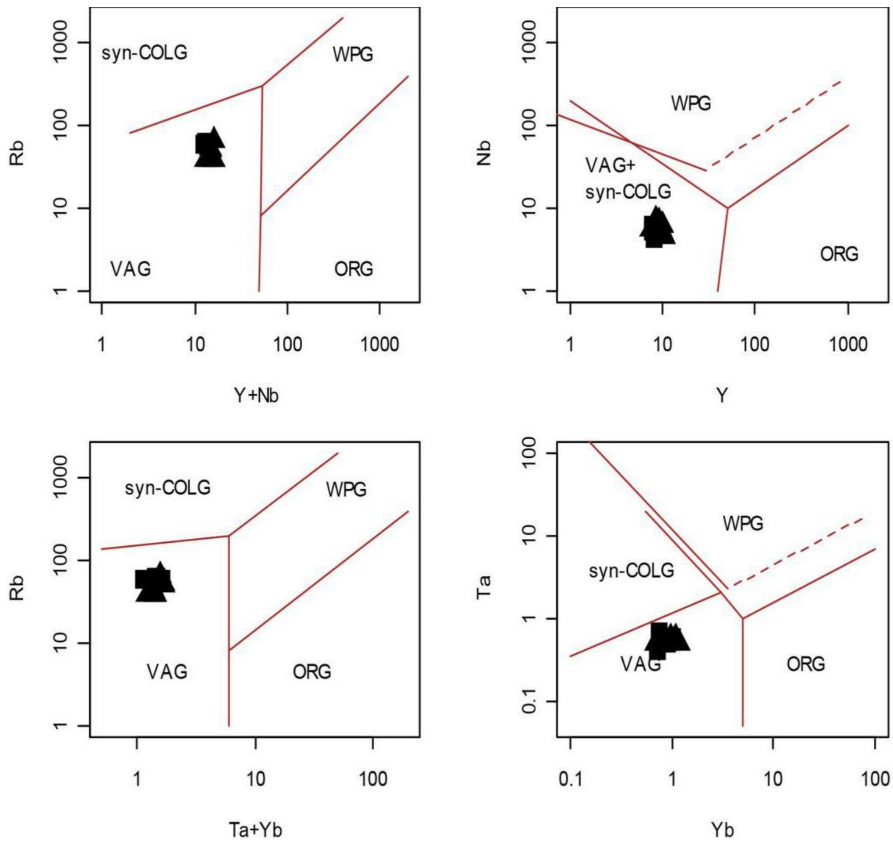

Figure 16) All samples plot in volcanic arc granite field (Pearce et al., 1984; Symbols is same as Fig. 3).

This petrologic family, termed *"adakites"*, was described by (Defant and Drummond, 1990) as high- alumina, intermediate to felsic volcanic rocks typically hosting phenocrysts of plagioclase, amphibole, mica and (rarely) orthopyroxene, and lacking phenocrysts of clinopyroxene. Accessory grains of titanomagnetite, apatite, zircon and titanite were identified as common but not ubiquitous (Defant and Drummond, 1990; Defant and Kepezhinskas, 2001., Martin *et al.*, 2004; Martin, and Hugh Rollinson, 2005). Also few adakitic plutons were reported (Martin, and Hugh Rollinson, 2005; Sengor and Natalin, 1996).

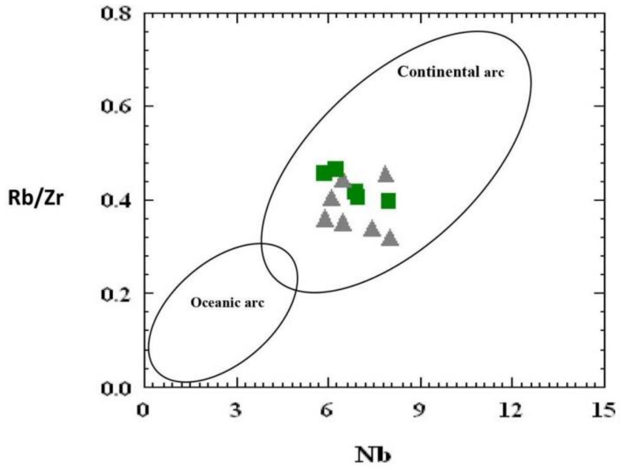

Figure 17) Nb vs. Rb/Zr diagrams, all of the samples plot in Continental arc, (Brown et al., 1984; Symbols is same as Fig. 3).

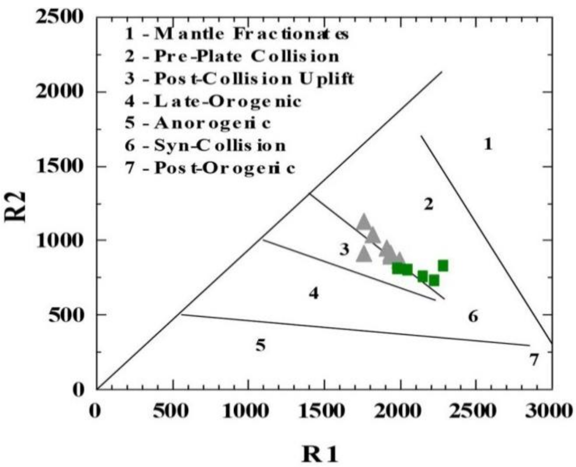

Figure 18) In Batchelor and Bowden, (1985) diagrams, all of the samples plot in Pre-Plate Collision Granite, [R1=4Si–11(Na+K)-2(Fe+Ti), R2=5Ca+2Mg+Al](Symbols is same as Fig. 3).

A complementary and broadly accepted chemical definition of adakites was sub-sequently provided: adakites are high-silica (SiO_2>56%), high-alumina (Al_2O_3>15%), plagioclase and amphibole-bearing lavas with Na_2O>3.5%, high Sr (>400ppm), low Y (<18ppm), high Sr/Y (>40), low Yb (<1.9), and high La/Yb>20 (Defant and Drummond, 1990; Defant and Kepezhinskas, 2001; Martin *et al.*, 2004; Martin, and Hugh Rollinson, 2005).

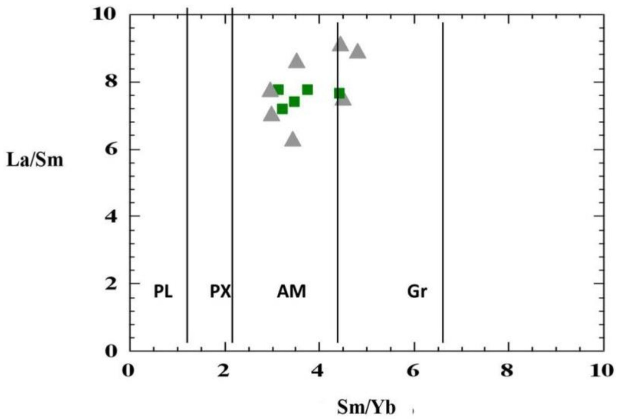

Figure 19) Sm/Yb vs. La/Sm diagram that show in mineralogy source rock of melting amphibol and garnet presented (Green et al., 1989; Kay and Mpodozis, 2002; Symbols is same as Fig. 3).

Geochemically, it appears that subduction related components played a controlling role in the genesis of the granitoidoides magmas in Central Volcanic Belt of Iran (CIVB). Enrichment of LILE and depletion of HFSE (Nb and Ti) and HREE are characteristic of subduction zone magmatism (Defant and Drummond, 1990; Defant and Kepezhinskas, 2001; Martin *et al.*, 2004). On the other hand the high ratios of Na_2O/K_2O, high Sr, Mg #, Sr/Y and $(Ce/Yb)_N$ suggest an adakitic character for subduction-related magmatism (Defant and Drummond, 1990; Defant and Kepezhinskas, 200; Martin *et al.*, 2004; Martin, and Hugh Rollinson, 2005).

The origin of adakites has been attributed to partial melting of either subducted oceanic crust converted to amphibole-eclogite and garnet-amphibolite (Defant and Drummond, 1990) or underplating of basaltic magmas under thick continental crust (Atherton and Petford, 1993).

The strongly fractionated REE pattern and depletions HREE and Y in adakites in this area are possibly due to the presence of garnet +/-

amphibole in melt residue. Their high Sr and low Nb, Ta, and Ti contents are thought to be due to absence of plagioclase and presence of Fe-Ti oxides in the residue (Martin, and Hugh Rollinson, 2005). While geochemical data for igneous rocks compiled by (Defant and Drummond, 1990) indicate a relationship between subducted oceanic crust and adakite genesis, adakite occurrences in different tectonic environment lad (Maury *et al.*, 1996) to propose that slab melting even of old oceanic crust is also possible during: 1- The initiation of subduction (Sajona, *et al.,* 2000). 2- Fast and oblique subduction (Peacock, 1996; Peacock *et al.,* 1994). 3- Termination of subduction (Sajona, *et al.,* 2000).

The high Mg and Cr content of most adakites are not consident with the low concentration of these elements in experimentally produced melts of amphibolite or eclogite. Sen and Dunn (1995) were atributed this enrichment to interaction of adakitic magma with the mantle during magma ascending. Experimental works by show that small amounts of adakitic melts are entirely consumed in reaction with mantle peridotite to from metasomatised zones as has been proposed by Rapp, *et al.,* (1999). On the other hand, when the ratio of melt/peridotite reaches 2:1, a portion of melt not consumed in the reaction becomes Mg-enriched and preserves its trace-element geochemical characteristics such as high Sr/Y and $(Ce/Yb)_{\mathbf{N}}$ ratios (Derek *et al.*, 2004).

The highly enriched N-MORB normalized abundance patterns of trace elements and REE pattern for the adakitic tonalite and granodiorite rocks of CIVB (area of Javazm, Khabr and Dehaj) suggest the existence of garnet as a residue in the source. In tonalite and granodiorite studied rocks the enrichment of Sr and the absence of negative Eu anomalies indicate that the residual source was pelagioclase free. The Nb and Ti are strongly depleted in the studied samples, which suggest that the source also has residual rutile and amphibole. Low abundances of HREE in granodiorites and tonalities rocks reflect retention of these elements in residual garnet in the partially melted subducted slab of amphibole-eclogite (Green *et al.*, 1989). Thus the source rocks of tonalites and granodiorites studied were most probably garnet-amphibolite or amphibole-eclogite. This garnet-bearing source implies that there are at least two possibilities for generation of adakitic tonalite and granodiorite rocks in Central Iran:

1. Partial melting of thickened lower crust and

2. Melting of subducted oceanic slab of Neo-Tethys as explained in below:

- It is expected that crustal thickening caused by Arabian-Asian continental collision would result in transformation of basaltic lower crust in to garnet-amphibolite or amphibole-eclogite. However, such deeper crustal materials have not been observed nor reported as xenolites from the studied area. Moreover, according to the Moho depth map of Dehghani and Makris (1984), the crustal thickness of the area ranges from 48 to 50Km. A seismic refraction profile through Sar-Cheshmeh, however gave crustal thicknesses of only 30 to 40 Km for the CIVB in Kerman province, which is not an adequate depth for conversion of basaltic lower crust in to garnet-amphibolite or amphibole-eclogite (Giese *et al.*, 1983).

- The other candidate hydrous amphibole-eclogite or garnet-amphibolite, which could melt to generate adakitic magmas in central Iran, is subducted Neo-Tethyan oceanic slab. The tonalite and granodiorite of study area show high Na_2O/K_2O, high Sr, low Y, strongly high REE depletion and high LREE. Peccerillo and Taylor (1976); White and Chappel (1983); Willson (1989) belive that such compositional bihaviour is consistent with their generation by melting of subducting oceanic lithosphere. The values of radiogenic Sr^{87}/Sr^{86} (0.704260 to 0.704443) for this rocks from respectively indicate that pelagic sediment could not have been involved in the genesis of the tonalite and granodiorite rocks (Ghadami, 2009). In tonalite and granodiorite studied rocks the enrichment of Sr and the absence of negative Eu anomalies indicate that the residual source was pelagioclase free. The Nb and Ti are strongly depleted in the studied samples, which suggest that the source also has residual rutile and amphibole. Partial melting of an amphibole-eclogite source would generate melts that have high Sr/Y, high LREE, but low Nb, Y, Yb, Ti and low HREE (Defant and Drummond, 1990; Defant and Kepezhinskas, 2001; Martin *et al.*, 2004). On the other analytical results show granitoides rocks of studied area that formed in a volcanic arc or an active continental margin related to subduction zone.

Controversy exists in the literature about the timing of the closure of Neo-Tethyan along the Zagros suture. Some authors infer late cretaceous age for continental collision (Berberian and King, 1981). A late Cretaceous age for continent-continent collision comes from the timing of the ophiolite emplacement, i.e.age of the youngest pelagic fossils involved in the Zagros ophiolites. However, this age has been shown to merely reflect the timing of ophiolite obduction due to collision of passive margin of Zagros-Oman an offshore intra-oceanic are (Dercourt *et al.*, 1986), while a vast area of oceanic lithosphere still existed to the north of Zagros yet to be subducted underneath central Iran during the Tertiary (Dercourt *et al.*, 1986). An alternative idea is that continental collision along the Zagros suture occurred in the Miocene (Sengor and Natalin, 1996).

Paleoceanographic constraints derived from carbon and oxygen isotopic date indicate that Neo-Tethys had a connection with the northern Indian Ocean until 14 Ma (Woodruff and Savin, 1989). This factor supports the Miocene reconstruction of Neo-Tethys by Sengor and Natalin, (1996) and is independent of regional geological evidence. Existence of widespread shallow marine and limited deep-marine Paleocene to Miocene sediment in Zagros sub-zones is consistent with the south arm of the Tethys remaining open in to Miocene (Mohajjel *et al.*, 2003). Opening of the Red Sea and the Gulf of Aden resulted in rotation of the Arabian plate with respect to Africa (Nubia ano Somalia) since 30 Ma (Hooper *et al.*, 1994; (Woodruff and Savin, 1989). This plate movement was responsible for oblique convergence between the Arabian plate and central Iran and final closure of Neo-Tethys (McCluske *et al.*, 2003).

Petrological studies carried out in this area and adjacent area i.e. Mosahim, Madvar, Aj Bala, and Aj Pain indicate that post collisional magmas exhibit various geochemical enrichment signatures (Hassanzadeh, 1993).

The significant character of post-colllisional magmatism in this area is progressive evolution of magmatic products from subalcaline to alkaline composition. A conspicous characteristic of alkaline phase is the contemporaneous of mafic alkaline melts including melafoides and alkali-basalts (Hassanzadeh, 1993).

Onset of magmatism in the late Miocene in this region with adakitic geochemical signatures, indicate the role of slab melting during of oblique convergence. Shear stress of oblique convergence could producted heating in the upper part of the subducted lithosphere (Peacock, 1996; Peacock *et al.*, 1994). The temporal and spatial relationship of the studied adakitic rocks may be attributed to oblique convergence subducted Neo-Tethyan oceanic lithosphere beneath the Central Iranian continental microplate (McCluske *et al.*, 2003). Thermal perturbation resulting in oblique convergence (Peacock, 1996; Peacock *et al.*, 1994) melting of detached slab and metasomatism of the mantle. The values of radiogenic Sr^{87}/Sr^{86} (0.704260 to 0.704443) and $\acute{\varepsilon}_{\mathbf{Nd}}$ (+1.3 to +1.4) for this rocks (Ghadami, 2009), respectively indicate fractionation and crystallization processes were involved (Moradian, 1997) this isotopic composition are similar to adakites from slab drived or MORB source (Derek *et al.*, 2004; Martin *et al.*, 2004).

3.2- Conclusions

(1) In central Iran (apart of volcanic belt of Iran) numerous plutonic masses of tonalite and granodiorite were intruded into different rocks during the Mio-Peliocene. They exhibit prophyritic texture with pheocrysts of plagioclase, hornblende and minor biotite.

(2) The geochemical characteristics of subalkaline tonalite and granodiorite rocks include high LILE, LREE, Sr, strongly fractionated REE patterns and low content of HREE and Y, in the diagram of Y vs. Sr/Y and the diagram of $(La/Yb)_N$ vs. Yb_N showing similarities with adakites.

(3) In this diagram of tectonic setting, adakitic granitoides of study area are I-typ and belong to VGA (volcanic granite arc), also this rocks had been formed in active continental margin.

(4) In tonalite and granodiorite studied rocks the enrichment of Sr and the absence of negative Eu anomalies indicate that the residual source was pelagioclase free. The Nb and Ti are strongly depleted in the studied samples, which suggest that the source also has residual rutile and amphibole. Low abundances of HREE in granodiorites and tonalities rocks reflect retention of these elements in residual garnet in the partially melted subducted slab of amphibole-eclogite.

(5) Garnet-amphibolite or amphybol-eclogite had been formed from subducted of Neo-Tethys bneath of centeral Iran during of Neogen.

(6) The isotopic chracteristices show the source of granitoides related to MORB.

(7) Thermal need for subducted slab melting products from thermal shear stress of oblique convergence between Neo-Tethys subduction in the volcanic belt of Iran in Miocene.

Acknowledgments

This research is based on field and laboratory studies carried out University of Hormozgan. I wish to acknowledge the kind support of the staff of this University.

References

Alavi, M. 2004. Regional stratigraphy of the Zagros fold-thrust belt of Iran and its proforeland evolution, American journal of Science: 304, 1–20.

Amidi, S. M., Emami, M. H., Michel, R. 1984. Alkaline character of Eocene volcanism in the middle part of Iran and its geodynamic situation. Geologische Rundschau: 73, 917–932.

Atherton, M. P., Petford, N., 1993. Generation of sodium-rich magmas from newly undererplated basaltic. Nature: 362, 144–146.

Batchelor, R. A., Bowden, P. 1985. Petrogenetic interpretation of granitoid rock series: using multinational parameters. Chemical Geology, 48: 35–55.

Berberian, F., Berberian, M. 1981. Tectono-plutonic episodes in Iran. In Gupta, H. K., Delany, F. M. (Eds.), Zagros, Hindukosh, Hymalaya, Geodynamic Evolution. American Geophysical Union, Washington, DC: 5–32.

Berberian, M., King, G. C. 1981. Towards a paleogeography and tectonics evolution of Iran. Canadian Journal of Earth Sciences: 18, 210–265.

Brown, G. C., Thorpe, R., Webb, P. C. 1984. The geochemical characteristics of granitoids in contrasting arcs and comments on magma sources. Journal Geological Society, London: 141, 413–426.

Chung, S. L., Chu, M. F., Zhang, Y., Zie, Y., Lo, C. H., Lee, T. Y., Ching-Ying Lan, C.Y., Xianhua Li, X., Zhang, O., Wang, Y. 2005.

Tibetan tectonic evolution inferred from spatial and temporal variations in post-collisional magmatism, Earth Sciences Review: 68, 173–198.

Condie, K. C. 1989. Geochemical changes in basalts and andesites across the Archean-Proterozoic boundry: identification and significancse. Lithos: 23, 1–18.

Cox, K. G., Bell, J. D., Pankhurst, R. J. 1979. The interpretation of igneous rocks. George Allen and Vnwin, London: 235p.

Dehghani, G. A., Makris, T. 1984. The gravity field and crustal structure of Iran. Neues Jahrbuch fur Geologie und Palaontologie-Abhandlungen: 168, 215–229.

Defant, J., Drummond, S. 1990. Derivation of some modern arc magmas by melting of young subducted lithosphere. Nature: 374, 662–665.

Defant, M. J., Kepezhinskas, P., 2001. Evidence suggests slab melting in arc magmas. EOS Trans., 20. American Geophysical Union,, Washington, DC: 82, 67–69.

Dercourt, J., Zonenenshain, L., Ricou, L. E., Kazmin, G., Lepichon, X., Knipper, A. L, Grandjacquet, C., Sbotshikov, I. M., Geyssant, J., Lepvrier, C., Pechersky, D. H., Boulin, J., Sibuet, J. C., Savostin, L. A., Sorokhtin, O., Westphal, M., Bazhenov, M. L., Lauer, J. P., Biju-Duval, B. 1986. Geological evolution of the Tethys belt from the Atlantic to Pamirs since the Lias. Tectonophysics: 123, 241–315.

Derek, J., Thorkelson., Kartin, B. 2004. Partial melting of slab window margins: genesis of adakitic. Lithos: 79, 25–41.

Dimitrijevic, M. D., Dimitrijevic, M. N., Djordjevic, M., Djokovic, I. 1971. Geological Survey of Iran, 1:100,000 Series: Sheet 7250, Anar.

Ghadami, G. R., Moradian, A., Mortazavi, M., 2008. Post-Collisional Plio-Pleistocene Adakitic volcanism in Centeral Iranian Volcanic Belt: Geochemical and geodynamic implications. Journal of Sciences, Islamic Republic of Iran, 19: 223–236.

Ghadami, G. R. 2009. Petrography, geochemistry and petrogeneses of intrusive and subvolcacies masses (adakitic) in Northwest Share-Babak, Kerman. Unpublished Ph.D. Thesis, Shaheed Bahonar University of Kerman, Islamic Republic of Iran, 334p.

Ghasemi, A., Talbot, C. J. 2006. A new tectonic scenario for the Sanandaj-Sirjan Zone (Iran). Journal of Asian Earth Sciences: 26, 683–693.

Gill, J. B. 1981. Orogenic andesites and plate tectonics, Springer Verlag, Berlin: 390p.

Giese, P., Makris, J., Akashe, B., Rower, P., Letz, H., Mostaanpour, M. 1983. Seismic crustal studies in southern Iran between the central Iran and Zagros belt. Geodynamic Project (Geotraverse) in Iran (Final report). Geological Survey of Iran, Report: 51, 71–88.

Green, T. H., Sie, S. H., Ryan, C. G., Cousense, R. D. 1989. Proton microprobe-determined partitioning of Nb, Ta, Zr, Sr, and Y between garnet, clinopyroxene and basaltic magmas at high pressure and temperature. Chemical Geology: 74, 201–216.

Haschke, M. R., Guenther, A. 2003. Balancing crustal thickening in arcs by tectonic vs. magmatic means. Geology: 31, 933–936.

Hassanzadeh, J. 1993. Metallogenic and tectonomagmatic events in the SE sector of the Cenozoic active continental margin of Iran (Shahre-Babak area, Kerman Province). Unpublished Ph. D thesis, University of California, Los Angeles: 204p.

Hooper, R. J., Baron, I., Hatcher, J. R. R. D., Agah, S., 1994. The development of the southern Tethyan margin in Iran after the break up of Gondwana: implications of the Zagros hydrocarbon province. Geosciences: 4, 72–85.

Irvine, T. N., Baragar, W. R. A. 1971. A guide to the chemical classification of the common volcanic rocks. Canadian Journal of Earth Sciences: 8, 523–548.

Jahangiri, A. 2007. Post-collisional Miocene adakitic volcanism in NW Iran: Geochemical and geodynamic implications, Journal of Asian Earth Sciences: 30, 433–447.

Jung, D., Kursten, M., Tarkian, M. 1976. Post-Mesozoic volcanism in Iran and its relation to the subduction of the Afro-Arabian under the Eurasian plate, In: Pilger, A., Rosler, A. (Eds.), A far Between Continental and Oceanic Rifting. Schweizerbartsche verlagbuchhand-iung Stuttgart: pp. 175–181.

Kay, S. M., Mpodozis, C. 2002. Magmatism as a probe to Neogene shallowing of the Nazca plate beneath the modern Chilean flat-slab. Journal of South American Earth Sciences: 15, 39-57.

Le Maitre, R. W., Bateman, P., Dudek, A., Keller, J., Le Bas, M. J., Sabine, P. A., Schmid, R., Sorensesen, H., Streckeisen, A., Woolley, A. R., Zanettin, B. A. 1989. Classification of Igneos Rocks and Glossary of Terms, Blackwell, Oxford: 193p.

Maniar, P. D., Piccoli, P. M., 1989. Tectonic discrimination of granitoids. Geological Society of America Bulletin: 101, 635–643.

Martin, H., Smithies, R. H., Rapp, R., Moyen, J. F. Champion, D. 2004. An overview of adakite-tonalite-trondhjemite-granodiorite (TTG), an Sanukitoid: relationships and some implications for crustal evolution. Lithos: 79, 1–24.

Martin, H., Rollinson, H. 2005. Geodynamic controls on adakite, TTG and Sanukitoid genesis: implications for modeles of crust formation. Lithos: 79, 1–4.

Maury, R. C., Sajona, F., Pubellier, M., Bellon, H., Defant, M. 1996. Fusion de la croute oceanique dans las zones de subduction/collision recentes: l' example de Mindanao (Philippines). Bulletin de la Societe Geologique de France: 167, 579–595.

McCluske, S., Balassanain, S., Baraka, A., Dmir, C., Ergintav, I., Gurkan, O., Hamburger, M., Hurst, K., Kahle, H., Kastens, K., Kekelidze, G., King, R., Kotzev, V., lenk O., Mahmoud, S., Nadariya, M., Ouzounis. A., Toksoz, M. N., Veis, G. 2003. Global positioning system constrains on plat Kinematics and dynamics in the eastern Mediterranean and Caucasus. Journal Geophys. Research: 105, 5695–5719.

Mohajjel, M., Fergusson, C. L., Sahandi, M. R. 2003. Cretaceous-Tertiary convergence and continental collision, Sanandaj-Sirjan Zone, western Iran. Journal of Asian Earth Sciences: 21, 397–412.

Moradian, A. 1997. Geochemistry, Geochronology and petrography of Feldspathoid Bearing Rocks in Urumieh-Dokhtar Volcanic Belt, Iran Unpublished Ph. D thesis, University of Wollongong, Australia: 412p.

Oyarzun, R., Marques, A., Lillo, J., lopez, I., Rivera, S., 2002. Gant versus small porphyry copper deposits of Cenozoic age in northern Chile: adakitic versus normal calc-alkalin magmatism. Mineral. Deposita: 36, 794–798.

Peacock, S. M. 1996. Thermal and petrologic structure of subduction zones. In: Bebout, G.E., Scholl, D.W., Kirby, S.H., and Platt, J.P. (eds.), Subduction: Top to Bottom. American Geophysical Union, Washington, DC, Geophys. Mon: 96, 119–133.

Peacock, S. M., Rushmer, T., Thompson, A. B., 1994. Partial melting of subducting oceanic crust. Earth and Planetary Science Letters: 121, 224–227.

Pearce, J. A. 1982. Trace element characteristics of lavas from destructive plate boundaries, In: Trop R.S.ed. Orogenic andesite and related rocks. John Wiley and Sons Chichester: 524–548.

Peccerillo, A., Taylor, S. R. 1976. Geochemistry of Eocene calc-alkaline volcanic rocks from the Kastamonu area, northern Turkey. Contributions to Mineralogy and Petrology: 58, 63–81.

Pearce, J. A., Parkinson, I. J. 1993. Trace element models for mantle melting: application to volcanic are petrogenesis. In: Prichard, H. M., Albaster, T., Harris, N. B. W., Neary, C. R. (Eds.), Magmatic Processes in Plate Tectonics: vol. 76. Geological Society of London Special Publication: pp 373–403.

Rapp, R. P., Shimizu, N., Norman, M. D., Applegate, G. S. 1999. Reaction between slab-derived melts and peridotite in the mantle wedge: experimental constraints at 3.8 GPa. Chemical Geology: 160, 335–356.

Reagan, M. K., Gill, J. B. 1989. Coexisting calc-alkaline and high niobium basalts from Turrialba volcano, Costa Rica: implications for residual titanates in arc magma sources. Journal of Geophysical Research: 94, 4619–4633.

Reich, M., Parada, M., Palacios, C., Dietrich, A., Schultz, F., Lehman, B. 2003. Adakite-like signature of Late Miocene intrusions at the Los Pelambres giant porphyry copper deposit in the Andes of central Chile: metallogenic implications. Mineral. Deposita: 38, 876–885.

Rollinson, H. R. 1993. Using Geochemical Data: Evalution, Presentation, Interpretation. Longman Geochemistry Series, 304p.

Sajona, F. G., Maury, R. C., Publlier, M., Letirrier, J., Bellon, H., Cotton, J. 2000. Magmatic source enrichment by slab-derived melts in a young post-collision setting, Central Mindanao (Philippines), Lithos: 54,173–206.

Sen, C., Dunn, T. 1995. Experimental modal metasomatism of a spinel lherzolite and production of amphibole-bearing peridotite. Contributions to Mineralogy and Petrology: 119, 422–432.

Sengor, A. M. C., Natalin, B. A. 1996. Paleotectonic of Asia: fragments of a synthesis. In Yin, A., Harrison, T. M., (Eds.), The Tectonic Evolution of Asia Combridge University Press, Cambridge: 486–640.

Shahabpour, J. 2007. Island-arc affinity of the Central Iranian Volcanic Belt. Journal of Asian Earth Sciences: 30, 652–665.

Sun, S. S., McDonough, W. F. 1989. Chemical and isotopic systematics of oceanic basalts: implications for mantle composition and processes. In: Saunders, A. D., and Norry, M. J., (Eds.), magmatism in ocean basins. Geological Society, London, Special Publication: 42, 313–345.

Tatsumi, Y., Koyaguchi, T. 1989. An absarokite from a phlogopite-lherzolite source. Contribution Mineralogy and Petrology: 102, 34–40.

White, A. J. R., Chappel, B. W. 1983. Granitoid types and their distribution in Lachlan fold belt, southeastern Australia. In: Roddick, J.A., (Ed.), Circum-Pacific plutonic terrains. Geological Society of America Memorial: 159, 21–34.

Willson, M. 1989. Igneous Petrogenesis: Global Tectonic Approach. Harper Collins Academic: 466p.

Woodruff, F., Savin, S. M. 1989. Miocene deep water oceanography. Paleoceanography: 4, 87–140.